Reinhard-illumination Based Single Scale Retinex for Low Light Images Amelioration

Manar Abdulkareem Al-Abaji and Mohammed Hazim Alkawaz *

Department of Computer Science, College of Education for Pure Science, University of Mosul, Nineveh, Iraq
Email: manar_alabaji@uomosul.edu.iq (M.A.A-.A.); mohammed.ameen@uomosul.edu.iq (M.H.A.)
Corresponding author

***Abstract*—Smartphones and digital cameras are essential tools for taking color images. Nevertheless, under poor lighting conditions, obtaining high-quality color images is difficult due to low brightness and uneven lighting. Various strategies have been suggested to enhance image light quality. Nevertheless, they did not produce a good result in the terms of excessive colors, halos, and loss of vital information. Therefore, the Reinhard-Illumination Based Single Scale Retinex (RISSR) algorithm is proposed in this study. The first step of the proposed algorithm involves inputting the degraded image and then predicting a single illumination map for all color channels which are altered using the Global Reinhard operator. In turn, the enhanced illumination is used to generate better color channels which are concatenated into the color image. This image is then processed with a gamma correction function and a normalization function to obtain the final improved image. The performance of the proposed algorithm was evaluated from real images under low-light conditions and judged by five metrics by comparison with ten other algorithms. Results indicated that the model presented the advantage of using the proposed algorithm with natural colors and perceived visual quality.**

***Keywords*—single scale Retinex, global Reinhard operator, low-light images, image enhancement, gamma correction**

I. INTRODUCTION

Most imaging and computer vision applications rely on high-quality images for efficient visual performance [1]. Images taken in dark and dim conditions like cloudy weather, night, and indoor illumination have low light, low contrast, and colors and therefore do not really reflect the actual scene and therefore affect image detail clarity. The images of such imaging images will contain considerable dark regions, so that they come out mostly dark, negatively affecting the performance of several image processing scenarios which are also widely used [2, 3]. This point indicates that applications for dark or shadowy image enhancement are particularly important for effectively revealing information and details through the light [4], thus better understanding, interpretation, and subsequent analysis [5]. Low-light image enhancement has a basic objective of producing clear, crisp, detailed, and high-quality images with no adverse side effects [6]. Although a lot of research has been done on the subject, few studies have been successful, the quality of the research varies often; hence, this field of research continues to develop. This has led several researchers to conduct research to tackle this issue and design algorithms with better processing power and output.

Accordingly, Fu *et al*. [7] propose a Fusion-based Enhancing (FE) technique for improving the weak-illumination images. The approach firstly decomposes the input image into illumination and reflectance using a morphological closing-based illumination estimation algorithm. Two new illumination forms (better contrast and luminance) generated by adaptive histogram equalization and a sigmoid function were then constructed, respectively. From the new versions, two different weights were created. The fusion of these versions in multi-scale fusion was further used for light-up adjustments by merging them with the weights. Finally, the modified vision is obtained by recombining the adjusted illumination with the original reflectance [7]. However, it tends to produce noticeable color distortion with unusual contrast. Yu and Zhu [8] report on the degradation of low-light images with a new Physical Lighting Model (PLM). This model depends on two principal components (rate of light-scattering attenuation and environmental light) to estimate iterative tuning. Then re-pack using weighted guide filter leads to an image with good local detail, and low color distortion [8]. However, it tends to destroy the image colors and produce noticeable unwanted artifacts. Moreover, Ghosh and Chaudhury [9] propose an additional method called Fast Bright-Pass Bilateral Filtering (FBPBF) to estimate the illumination for enhancing the illumination in Retinex theory to improve the quality of dim images. This approach broadens the Fourier approximation and turns it into an efficient-fast, bright-pass bilateral filter. The possibility of rapid improvement of ill-lit images by the method has been tested in reports [9]. However, it added limited brightness and caused noise amplification. Concurrently, Wang *et al*. [10] design an adaptive approach to boosting the image brightness with the help of the Weber-Fechner Law. The illumination part was obtained with the

Manuscript received December 18, 2025; revised January 23, 2026; accepted March 13, 2026; published July 17, 2026.

multiscale Gaussian function employed through the V component after conversion of the Red Green Blue (RGB) image to the Hue, Saturation, Value (HSV) color space. Then, the Weber-Fechner law is used to construct a correction function, thus the two images, fused and their meaningful details are preserved [10]. However, the resultant image suffers from unbalanced brightness, leading to the generation of halos.

In addition, Hao *et al*. [11] proposes a novel poor-light image enhancing technique called Gaussian Total Variation (GTV) by semi-decoupled decomposition of the Retinex image. In such a method, the illumination component is estimated from the input image through the Gaussian total variation filter, and the reflectance component is estimated jointly from both the input image and the intermediate illumination component [11]. However, it results blow the required visual perception for specific image contents. Similarly, Hassan [12] developed a technique to enhance the low-light images through linear transformation construction of the lightness and chroma in the color space of International Commission on Illumination L*a*b* (CIELAB) (Uniform Illumination Enhancement (UIE)). There are two phases in this method: chrominance and luminance improvements. Chrominance enhancement essentially involves enhancement of the chroma as well as the chromaticity indices of the low-light pictures [12]. However, it produces insufficient contrast and untrue illumination equalization. Moreover, Hassan *et al*. [13] present an approach to boosting image light and preserving the color of the image using triangle similarity in the Hue-Saturation-Intensity (HSI) color space (TS) condition. The presented method consists of two stages. In the preceding step, the image intensity was improved after performing a linear translation operation. As a follow-up, image saturation was expanded in the second stage by scaling. The obtained final improved image was obtained while converting the HSI image to the RGB color space [13].

However, the resultant image suffers from low illumination with unwanted artifacts. Additionally, Demir and Kaplan [14] propose a novel technique to enhance image brightness using the Sharpening-Smoothing Image Filter (SSIF). In the HSV approach, the input image is mapped to the HSV color space. The details and approximation images for the V component were acquired by applying the SSIF multi-scale decomposition. The detailed image was amplified; the approximation image improvement was done with CLAHE. Next, the enhanced V was rebuilt and inversely transformed HSV was performed to obtain the final enhanced image [14]. However, it tends to produce a noticeable noise with unnatural brightness. Also, Wang *et al*. [15] propose a method to improve dim images. The method is based on a convolutional neural network with the Retinex theory to build a model consisting of decomposition, illumination, and reflectance modules. Firstly, the image is decomposed into the illumination and the reflectance using the decomposition module. After that illumination, reflectance modules are used for enhancing the feature extraction process and enhancing the texture details, respectively. Although the method can restore distinct contrast and good colors but it requires more computations [15].

Wang *et al*. [16] present an algorithm for dark-channel prior to improve low light images by combining the genetic algorithm with the quadtree segmentation. The haze version of the input image is segmented using the quadtree method, then the estimated light values were enhanced using the genetic algorithm, which led to improved image contrast. While the guided filter and morphological operation are used to refine the dark-channel image derived from the adaptive window size, enhancing the dehazing effect. Utilizing the genetic algorithm makes the presented algorithm unsuitable for real time application because of its high computational complexity [16].

In addition, Severoglu *et al*. [17] use Adaptive Chrominance Gamma Correction (ACGC) for the low-light images. This approach is based on the Luma-In-phase-Quadrature (Y-I-Q) transformation of enhancement with a bilateral filter in least squares to improve the transformation process. After using the Y-I-Q transform, the input image is fed through gamma correction. Used Bilateral Filter in Least Squares (BLF-LS) and Y-I-Q transform to transform the input image. BLF-LS of the Y component is passed to extract the latter to the low and the higher frequency layer. Local gamma correction followed by CLAHE is added to the low frequency with the high frequency layer on the high frequency layer, to get the amplitude-enhanced Y, I, and Q components, which were also enhanced, although using Local gamma correction. The image of the final image was constructed as per the inverse Y-I-Q transform [17]. However, the resultant image suffers from over-enhancing, which leads to pallid colors and improper contrast. Finally, Kucuk *et al*. [18] presents a novel approach for achieving low-light image quality by a novel color channel, based on a physical lighting model, and particularly their concept (NCC_PLM). Firstly, the procedure performs gamma correction on the selected image, based on its degree of darkness. The method then employed a physical lighting model for low light image detail recovery and to obtain the final enhanced image by estimating the light scattering attenuation rate and environmental light in the new color channel [18]. However, it excessively boosts image brightness which results in dull image colors. Several concepts have been applied to enhance image lighting, as identified by the methods and studies conducted in this review. Nevertheless, many of these approaches have led to large-scale distortions and faults, including extreme brightness amplification, over-smoothing, color shifts, improper adjustments, and costly computational efforts.

Accordingly, the demand for easy and efficient methods for better lighting of badly lit images is higher than ever, and this is what this research seeks to solve. Thus, a novel Reinhard-Illumination Based Single Scale Retinex (RISSR) algorithm was developed to process such mis-illuminated images under poor lighting. The critical aim here is to take better images with good light and light contrast, and image detail and information, and to maintain the color of images in accordance with traditional colors by use of a low-complexity and fast process. RISSR is based on the Retinex theory, which postulates that the output of an image is the product of the two key elements (light and reflection). This algorithm takes the max of the entire depth of the color channels of the image to produce the illumination, which are then convolved (*) into a discrete 2D Gaussian surround function. The estimated illumination is processed and adjusted to obtain better color channels via the global Reinhard operator. Then, these channels produce a colored image that can be processed further through gamma correction and a normalization function to reach the final enhanced image. The proposed algorithm's key contributions are: (i) The algorithm we propose is implemented on images, i.e., it does not need a bunch of the same scene images like those proposed by fusion-based algorithms. (ii) We think it has been the first model for optimization and its application on low-light images utilizing the Reinhard operator is also beneficial as it aims to enhance image lighting and image detail in dark regions. (iii) It operates on low-complexity operations for learning images.

The rest of this work is organized in that: Section II provides the history of the Reinhard Operator and Single Scale Retinex (SSR). Section III describes the introduction to the proposed algorithm. Performance evaluation with comparisons is presented in Section IV. Then, lastly, the conclusion is provided in Section V.

II. Technical Background

A. The Reinhard Tone Mapping Operator

Reinhard Tone Mapping Operator (TMO) was introduced by Reinhard *et al.* [19]. It's a simple tone mapping method that focuses primarily on how to set the brightness. Therefore, it's used to convert an image with a high dynamic range to a low dynamic range, which looks natural and is pleasing to the eye, just like a high-quality photograph [20]. The global Reinhard TMO can be done by analyzing the overall scene brightness, then all the pixel values scale relative to "key", which represents the log average brightness of the scene. Finally, a simple curve to compress the highlights is applied to get the enhanced image with brightness that feels right. The pixel value scales are given using the following Eq. (1) [21]:

$$L(x,y) = \frac{\alpha}{L_{\log\_av}} L_{in}(x,y) \tag{1}$$

where L_{in} is the input pixel luminance, α is a parameter that allows the user to map the log average brightness of the scene to various values of α, $L_{\log\_av}$ is the log average brightness, which can be defined using Eq. (2):

$$L_{\log\_av} = \exp\left(\frac{1}{N}\sum_{x,y}\log\left(\delta + L_{in}(x,y)\right)\right) \tag{2}$$

where N is the total number of pixels, δ is a small value, $\delta > 0$, to prevent the singularity that happens when there are black pixels in the image. Finally, the mapping operator is given using the following Eq. (3):

$$L\_new(x,y) = \frac{L(x,y)}{1+L(x,y)} \tag{3}$$

Overall, the Reinhard operator results in good images for high and standard dynamic range. Because it utilized a photographic technique for both dodging and burning, which resulted in enhancing the images' dynamic range and its overall quality. In addition, the Reinhard operator efficiently reveals image details and information in dark areas while improving contrast and brightness [19].

B. The Single Scale Retinex Algorithm

SSR was introduced by Jobson *et al.* [22], who characterized it by its low computational cost and potential for improving image lighting. In the SSR model, illumination is estimated by convolve (*) the degraded image P (x, y) with a discrete 2D Gaussian surround function G (x, y). The logarithms of the resulting illumination image and the degraded image are then calculated. The reflection image R (x, y) is then found by subtracting the log of the illumination image from the log of the degraded image; the result represents the image with improved illumination [23]. The illumination image is estimated using the following Eqs. (4) and (5):

$$G_{(x,y)} = K \cdot \exp^{-\frac{V^2+H^2}{2\sigma^2}} \tag{4}$$

$$K = \frac{1}{\sum_{i=1}^{N}\sum_{j=1}^{M}\exp^{-\frac{\left(V^2+H^2\right)}{2\sigma^2}}} \tag{5}$$

where K is the normalization factor, x and y represent the image coordinates, V and H represent two gray gradients (vertical and horizontal), image dimensions represented by N and M, × signifies a multiplication operator, σ is a scalar to control image illumination ($\sigma > 1$). After that, the reflectance image (improved image) obtained using the following Eq. (6) [24]:

$$R_{(x,y)} = \log\left[P_{(x,y)}\right] - \log\left[G_{(x,y)} \times P_{(x,y)}\right] \tag{6}$$

III. Research Method

A. Proposed Algorithm

The purpose of proposing the RISSR method is to improve images taken in unfavorable lighting conditions with high efficiency and low computational complexity and cost. Several concepts have been used previously for this purpose, including SSR. Although the SSR model is characterized by few calculations and a simple structure, it does not yield ideal results. It tends to increase brightness in bright areas of the image and further dim dark areas, leading to the loss of important image information and unnatural color reproduction. Therefore, it has attracted the attention of many researchers due to its simplicity, its close resemblance to the human visual system, and its potential for development.

Thus, in this study, the RISSR algorithm, based on the original SSR model with a Reinhard operator, was developed to enhance low-light images. The proposed algorithm optimizes low- and medium-density pixels while preventing excessive pixel density in high-density pixels, resulting in better color reproduction. The reason for incorporating the Reinhard operator is to improve the performance of the original SSR algorithm in enhancing dark areas while simultaneously preventing over-brightening of bright areas. The Reinhard operator employs an intelligent curve that adapts its shape based on the perceived brightness of the image. Eq. (1) represents an adaptive scaling process that is based on the log average brightness of the image. In the case of an image with a high dynamic range, it scales the image down to a normal level. While in the case of a low-light image, it scales it up, boosting or expanding the dark or shadowy pixels to perceived mid-tones. Eq. (3) is used for compresses the highlight pixels, preserving bright pixels in the images from becoming pure white (over-boosted) as a result of applying Eq. (1). This is very important in methods of improving dark images that contain well-lit areas to avoid increasing their brightness even further.

Initially, the low-light image is input, and a single illumination map (L_{in}) is estimated for all channels (red, green, and blue) by taking the max of R, G, and B as our intensity. Then, a discrete 2D Gaussian function is applied to it using Eq. (4). This optimizes all colors simultaneously and avoids color shift and fading. The global Reinhard operator is used to fine-tune the estimated illumination map to get (L_new) using Eq. (3). In this study, the value of sigma used is equal to ($\sigma = 80$) to suppress the special variations and preserve only the very low frequency image components, which represent the background or the illumination map of the image. After illumination adjustment, the reflectance for each channel is calculated separately. In the Retinex theory, the image was expressed as the multiplication of two components: illumination and reflection. Therefore, the reflectance of (R, G, B) can be obtained by dividing each color channel by image illumination as illustrated in the following Eqs. (7)–(9):

$$R_{\text{Red}} = \frac{channel_{\text{Red}}}{L_{in} + \varepsilon} \tag{7}$$

$$R_{\text{Green}} = \frac{channel_{\text{Green}}}{L_{in} + \varepsilon} \tag{8}$$

$$R_{\text{Blue}} = \frac{channel_{\text{Blue}}}{L_{in} + \varepsilon} \tag{9}$$

where $channel_{\text{Red}}$, $channel_{\text{Green}}$, $channel_{\text{Blue}}$ are three color channels for the low light image, L_{in} is the estimated illumination for all channels, ε is mini value ($\varepsilon = 0.001$) to exclude division by zero.

Then the reflectance for each channel was recombined with the adjusted illumination (L_new) to produce improved color channels, which are then concatenates to produce the color image (F). The following Eqs. (10)–(12) to calculate the improved color channels:

$$New\_channel_{\text{Red}} = R_{\text{Red}} \cdot L\_new \tag{10}$$

$$New\_channel_{\text{Green}} = R_{\text{Green}} \cdot L\_new \tag{11}$$

$$New\_channel_{\text{Blue}} = R_{\text{Blue}} \cdot L\_new \tag{12}$$

A gamma correction function is applied as a post-processing step to the resulting color image to control the level of detail enhancement and correct overexposed areas. The simple formula of gamma correction [17] is as Eq. (13):

$$F_1 = F_{\max} \left(\frac{F}{F_{\max}} \right)^{\gamma} \tag{13}$$

where F is the color image which is produced by concatenated improved color channels, F_1 represents the corrected image, $F_{\max}$ represents the maximum value in F, and γ is the gamma value. In this study, $\gamma = 1/1.3$, which brightens dark areas in images and increases its contrast. Finally, a linear normalization function that is illustrated in Eq. (14) is used to adjust all image pixel values within the dynamic range [25]. The output of this stage will be an enhanced image:

$$F_2 = \frac{F_1 - \min(F_1)}{\max(F_1) - \min(F_1)} \tag{14}$$

where F_2 is the output enhanced image, max and min represent the highest and lowest pixel values in F_1.

Pseudo-Code of the Proposed RISSR
Input: Low-light image P, parameter α
Calculate the max of R, G, and B
Estimate single illumination map (L_{in}) based on the max using Eq. (4)
Apply the Global Reinhard operator on (L_{in}) to obtain (L_new) using Eq. (3)
Calculate the reflectance of (R, G, B) using Eqs. (7)–(9)
Calculate the improved color channels (R, G, B) using Eqs. (10)–(12)
Apply the gamma correction function using Eq. (l3)
Compute the linear normalization function using Eq. (14)
Output: the enhanced image F_2

The pseudo-code and the block diagram in Fig. 1 illustrate the main operations and steps of the proposed algorithm for better understanding.

The performance of the proposed algorithm on degraded images is illustrated in Figs. 2 and 3 using different values of α. The value of α that yielded the best results in processing low-light images falls within the range of (0.1–1). When its value is low, the image brightness is low.

Furthermore, the choice of α value depends on the illumination nature of the image being processed. If the image is a nighttime image (extremely dark), a value of α close to 0.1 gives better results (image information becomes more visible with good contrast and brightness), while other low light images may require a value close to 1 to obtain a natural appearance with pleasant brightness. Therefore, the choice of a value is the user's responsibility, as a different value is set for each image individually to control its final appearance.

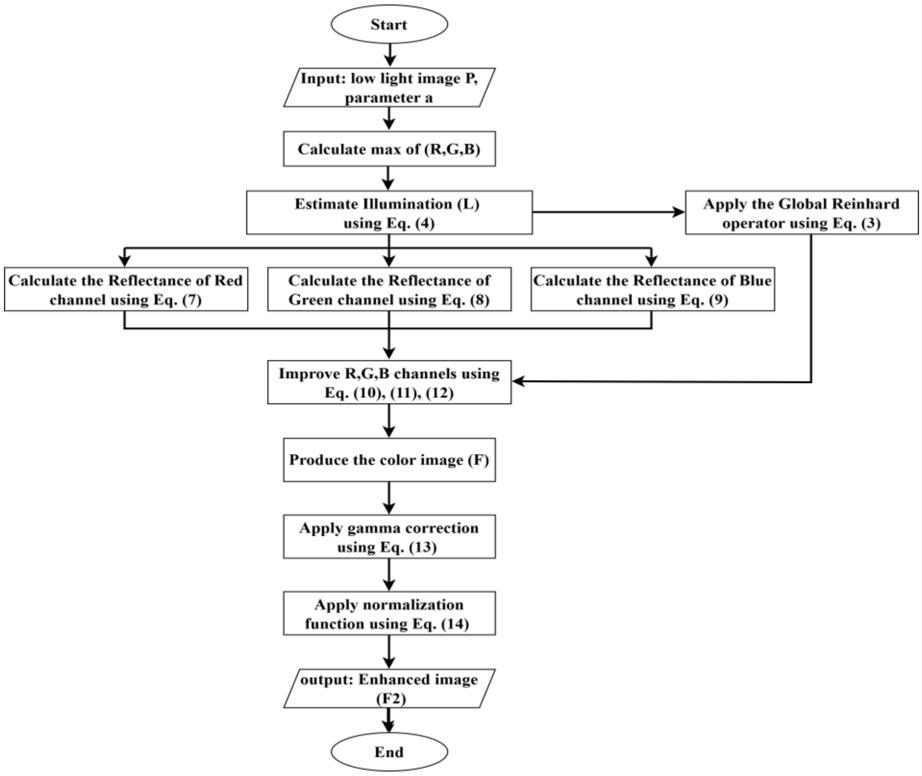

Fig. 1. The proposed RISSR block diagram.

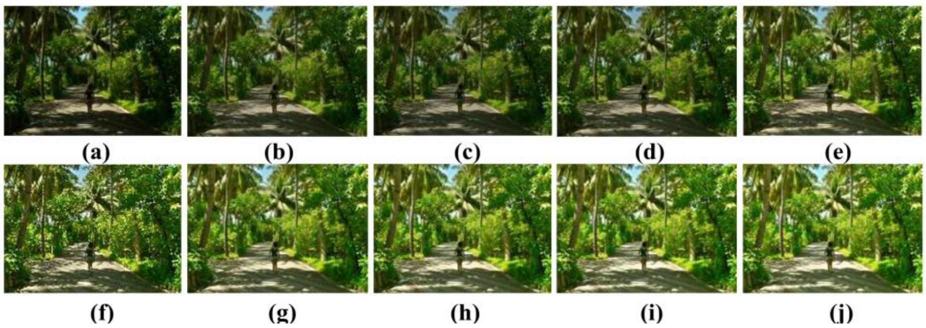

Fig. 2. Restored images by applying SISSR algorithm on low_light image using different value of α: (a) the degraded image, (b) $\alpha = 0.1$, (c) $\alpha = 0.2$, (d) $\alpha = 0.3$, (e) $\alpha = 0.4$, (f) $\alpha = 0.5$, (g) $\alpha = 0.6$, (h) $\alpha = 0.7$, (i) $\alpha = 0.8$, (j) $\alpha = 0.9$.

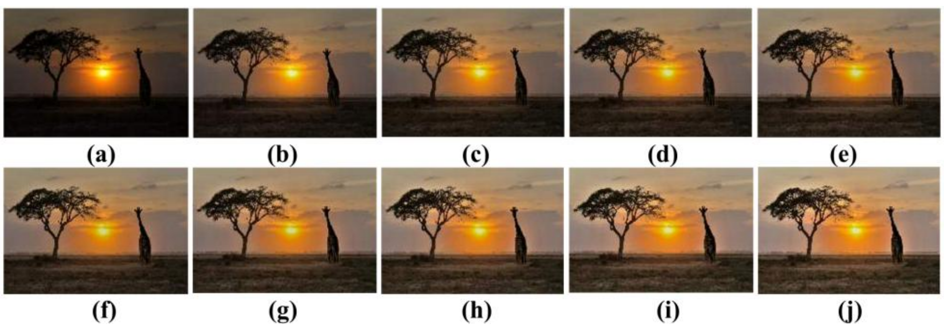

Fig. 3. Restored images by applying SISSR algorithm on another low_light image using different value of α: (a) the degraded image, (b) $\alpha = 0.1$, (c) $\alpha = 0.2$, (d) $\alpha = 0.3$, (e) $\alpha = 0.4$, (f) $\alpha = 0.5$, (g) $\alpha = 0.6$, (h) $\alpha = 0.7$, (i) $\alpha = 0.8$, (j) $\alpha = 0.9$.

B. Experiment Setup and Evaluation Metrics

This section contains all the data related to the experiments preparation to apply and the proposed algorithm. Several datasets were used, each containing images with actual degradation, including Flickr [26], Digital Image Collection for Multi-Exposure (DICM) [27], Multi-Exposure Fusion (MEF) [28], Exclusively Dark Dataset (ExDark) [29], and Low-Light Dataset (v1) (LOL-v1) [30] datasets. Also, the proposed algorithm was tested with a dataset collected from a website. All datasets contain real images taken in poor lighting conditions (cloudy weather, night lighting, and interior lighting) to demonstrate the effectiveness of the proposed algorithm in enhancing images under various lighting effects. The proposed algorithm was compared with ten other algorithms that are: Adaptive Chrominance Gamma Correction (ACGC) [17], PLM [8], FE [7], AIE [10], UIE [12], TS [13], FBPBF [9], NCC_PLM [18], LightenNet [31], Low-Light Image Enhancement via Illumination Map Estimation (LIME) [32] and the results obtained were evaluated using three no-reference metrics that are, Blind Reference less Image Spatial Quality Evaluator (BRISQUE) [33], Perception-based Image Quality Evaluator (PIQE) [34], and a Novel Blind Image Quality Assessment (NBIQA) [35]. And evaluated using two full-reference metrics, that are, Peak Signal-to-Noise Ratio (PSNR), Structural Similarity (SSIM) [36]. Regarding the BRISQUE metric, used to measure the perceived visual quality of an image, it works by taking statistical properties from the image using a Gabor filter, then extracting the necessary coefficients to evaluate the image using a least squares model. A lower value on this metric indicates better perceived quality. The PIQE metric, on the other hand, relies on local image features to measure the degree of distortion. A low value indicates a lower visibility of the image distortion. NBIQA is used to predict image naturalness by analyzing uniquely collected statistical image characteristics from both domains (spatial and DCT). An enhanced NSS model is then built to feed the SVM technique for training a regression model that will be used to predict perceived image quality. A high value on this metric represents better image quality. Regarding PSNR and SSIM, the higher score in PSNR indicates better image quality, while the higher score in SSIM indicates more structural similarity between the images. As for implementing the proposed algorithm and conducting all experiments and comparisons, this was done using MATLAB 2023a.

IV. Results and Discussion

The section contains all the data related to the experiments and comparisons conducted on the proposed algorithm. Figs. 4–9 illustrate the results of applying the proposed algorithm to a set of low-light color images. It elucidates the ability of the proposed RISSR algorithm to ameliorate the perceived quality of color images taken in unsuitable lighting conditions by obtaining images with balanced lighting, good colors and contrast. It also improves the dark areas of the image and prevents excessive brightness in the bright areas, making the image details more perceptible without any distortions in the resulting images. In addition, it retains edge information and does not add a smoothing effect to the image, thus making it look more realistic. These outcomes are worthy because it produces visual pleasing images using a non-complex and fast algorithm with simple calculations.

Fig. 4. The outcomes of applying the proposed RISSR algorithm on low light images from Flickr dataset (Batch 1). The first row are the degraded images, the second row are the enhanced images using α = 0.6, 0.75, 0.8, 0.49, 0.68, respectively.

Fig. 5. The outcomes of applying the proposed RISSR algorithm on low light images from DICM dataset (Batch 2). The first row are the degraded images, the second row are the enhanced images using α = 0.87, 0.98, 0.91, 0.2, 0.1, respectively.

Fig.6. The outcomes of applying the proposed RISSR algorithm on low light images collected from the web (Batch 3). The first row are the degraded images, the second row are the enhanced images using α = 0.8, 0.78, 0.58, 0.7, 0.55, respectively

Fig. 7. The outcomes of applying the proposed RISSR algorithm on low light images from MEF dataset (Batch 4). The first row are the degraded images, the second row are the enhanced images using α = 0.75, 0.98, 0.52, 0.41, 0.73, respectively.

Fig. 8. The outcomes of applying the proposed RISSR algorithm on low light images from ExDark dataset (Batch 5). The first row are the degraded images, the second row are the enhanced images using α = 0.51, 0.72, 0.91, 0.59, 0.87, respectively.

Fig. 9. The outcomes of applying the proposed RISSR algorithm on low light images from LOL-v1 dataset (Batch 6). The first row are the degraded images, the second row are the enhanced images using α = 0.7, 0.68, 0.53, 0.62, 0.49, respectively.

A. Comparison 1

The first comparison used 300 low-light color images collected from four datasets and an additional website. Specifically, 80 images were obtained from Flickr, 64 from the DICM dataset, 17 from the MEF dataset, 100 from the ExDark dataset, and 39 images were collected from a website. And evaluated using three no-reference metrics, BRISQUE, PIQE, and NBIQA. Figs. 10–14 show the results of comparing the proposed algorithm with other algorithms. Tables I–IV present the recorded metric values and the processing time for the comparison. Table V presents the average metric scores (300 images) for all algorithms. Figs. 15–18 represent the results as averages in the form of graphs.The comparison noted that each algorithm yielded different results due to its reliance on different processing concepts. The analysis of each algorithm considers aspects such as contrast quality, colors, detail sharpness, and light balance. In addition to the occurrence of errors and artifacts. Therefore, observations regarding the performance of the algorithms were recorded. Some did not produce good results because it did not provide adequate processing of image properties related to colors, lighting, contrast, and detail sharpness, while others generated undesirable visual distortions. The ACGC algorithm produced images with washed-out colors, insufficient contrast, and noticeable distortions. This justifies obtaining very low scores with BRISQUE, very low scores with PIQE, and the worst with NBIQA metrics. Also, it ranked sixth in terms of processing speed. As for the PLM algorithm, it obtained the worst with BRISQUE, the worst with PIQE, and poor with NBIQA because it tends to produce images with significant color distortion and noticeable halos. It also had a very low processing time among the other algorithms. It had a slow execution time. Although the FE algorithm ranked fourth in processing, it added a limited brightness and noticeable color distortion to the resulting images. This explains why it received poor with BRISQUE, moderately with PIQE, and below moderate with NBIQA. The AIE algorithm achieved the shortest processing time but exhibited unnatural totality and unbalanced brightness, leading to halos in some areas of the restored image. It obtains high with BRISQUE, above moderate with PIQE, and the second best with NBIQA. The UIE algorithm added a moderate improvement to the image's brightness but with insufficient contrast, resulting in relatively dark images. It was also ranked as the tenth algorithm in terms of processing time. It gets the second best with BRISQUE, the second best with PIQE, and above moderate with NBIQA. As for the TS algorithm, it achieved low with BRISQUE, poor with PIQE, and very low with NBIQA. This is because the resulting images suffered from reduced brightness and increased smoothness. It was also ranked seventh in processing.

The FBPBF algorithm ranks eighth in computation time, provided sufficient contrast and good brightness but generated unwanted distortions. Therefore, it obtained below high with BRISQUE and NBIQA, and high with PIQE. Meanwhile, the NCC_PLM algorithm excessively increased brightness, resulting in relatively dull colors and visual image details. This justifies obtained value above moderate with BRISQUE, below high with PIQE, and high with NBIQA. Regarding processing speed, it ranks fifth. Although the LIME algorithm ranked third in terms of processing time, it adds extreme brightness amplification which led to the appearance of unwanted artifacts. This is why it received below moderate in BRISQUE, low in PIQE and NBIQA metrics. The LightenNet algorithm produces images with low illumination and tends to add halos in some images. Therefore, it obtained moderate in BRISQUE and NBIQA, and below moderate in PIQE. Also, it has the slowest processing time. As for the proposed RISSR algorithm, it outperformed its competitors, achieving the best values in the BRISQUE, PIQE, and NBIQA metrics. It also produced images with perceived visual quality, characterized by improved contrast, natural brightness, and vibrant colors. Furthermore, image details appeared sharp and clear. In addition, it improved the illumination of dark areas without introducing any distortion or noise amplification, which is crucial for developing a simple and computationally uncomplicated algorithm. Regarding processing speed, the proposed algorithm ranked second among the competing algorithms.

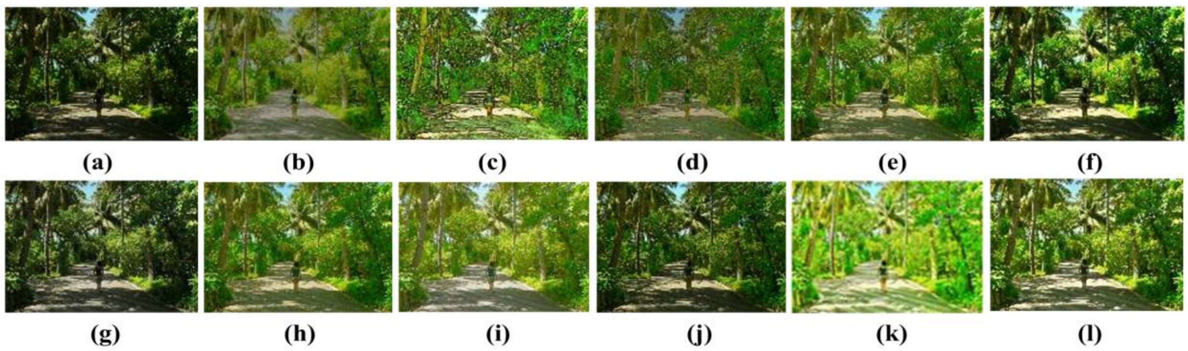

Fig. 10. Comparison outcomes of the Flickr dataset (Batch 1): (a) Original degraded image, (b) ACGC, (c) PLM, (d) FE, (e) AIE, (f) UIE, (g) TS, (h) FBPBF, (i) NCC_PLM, (j) LightenNet, (k) LIME, (l) the proposed RISSR algorithm.

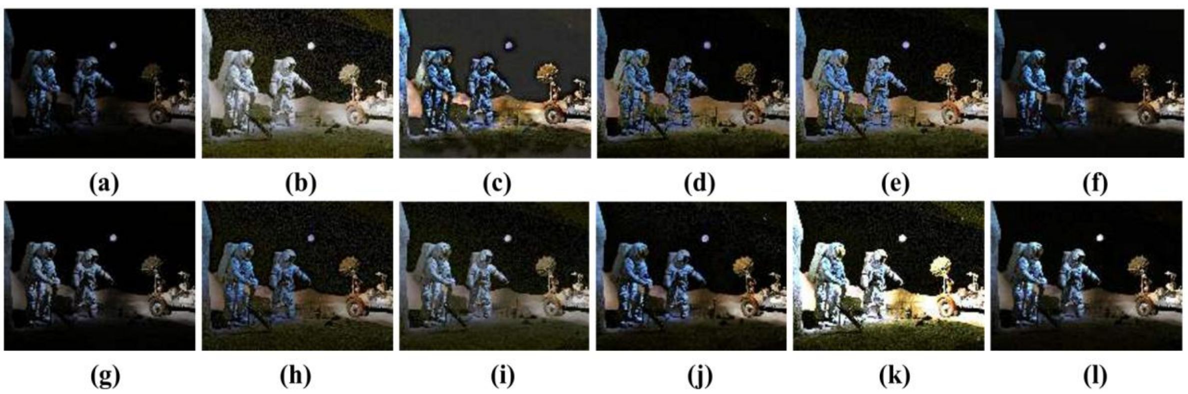

Fig. 11. Comparison outcomes of the DICM dataset (Batch 2): (a) Original degraded image, (b) ACGC, (c) PLM, (d) FE, (e) AIE, (f) UIE, (g) TS, (h) FBPBF, (i) NCC_PLM, (j) LightenNet, (k) LIME, (l) the proposed RISSR algorithm.

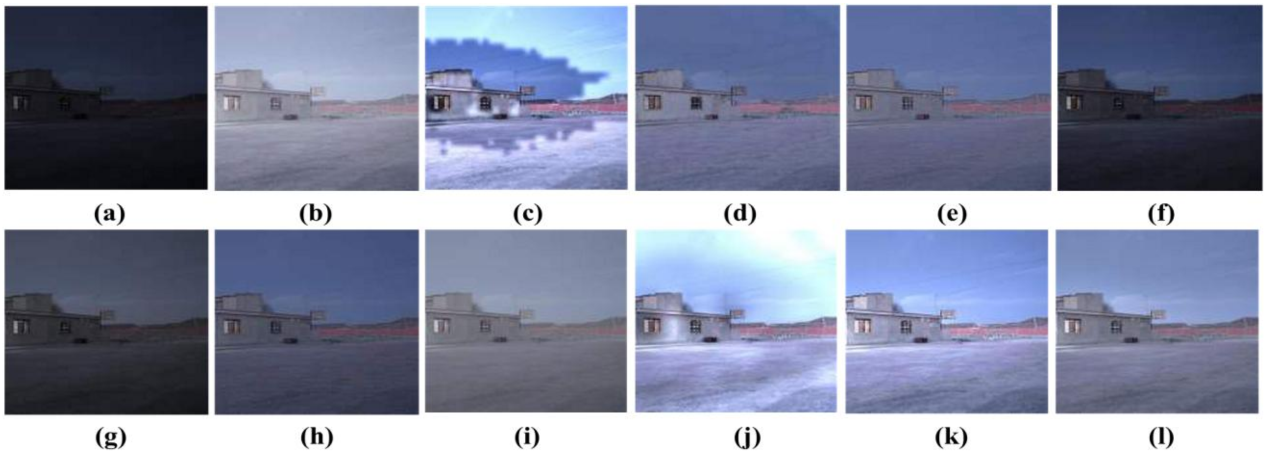

Fig. 12. Comparison outcomes of the dataset collected from the web (Batch 3): (a) Original degraded image, (b) ACGC, (c) PLM, (d) FE, (e) AIE, (f) UIE, (g) TS, (h) FBPBF, (i) NCC_PLM, (j) LightenNet, (k) LIME, (l) the proposed RISSR algorithm.

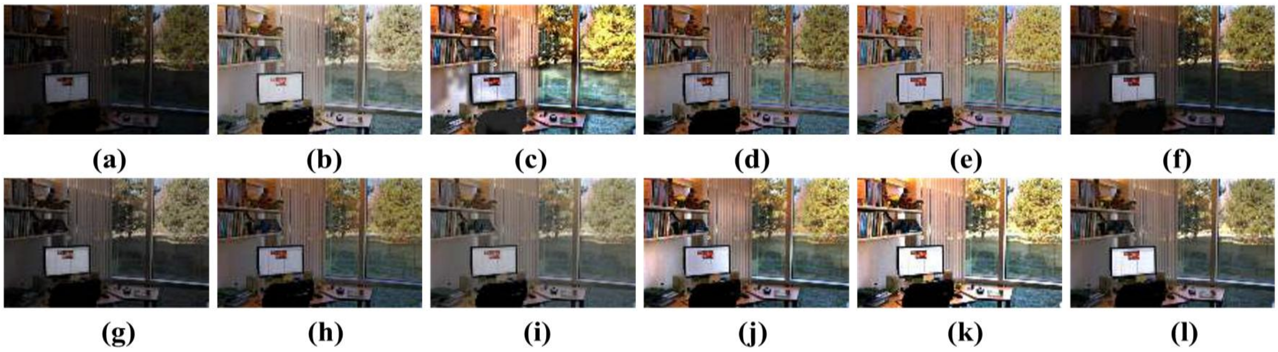

Fig. 13. Comparison outcomes of the MEF dataset (Batch 4): (a) Original degraded image, (b) ACGC, (c) PLM, (d) FE, (e) AIE, (f) UIE, (g) TS, (h) FBPBF, (i) NCC_PLM, (j) LightenNet, (k) LIME, (l) the proposed RISSR algorithm.

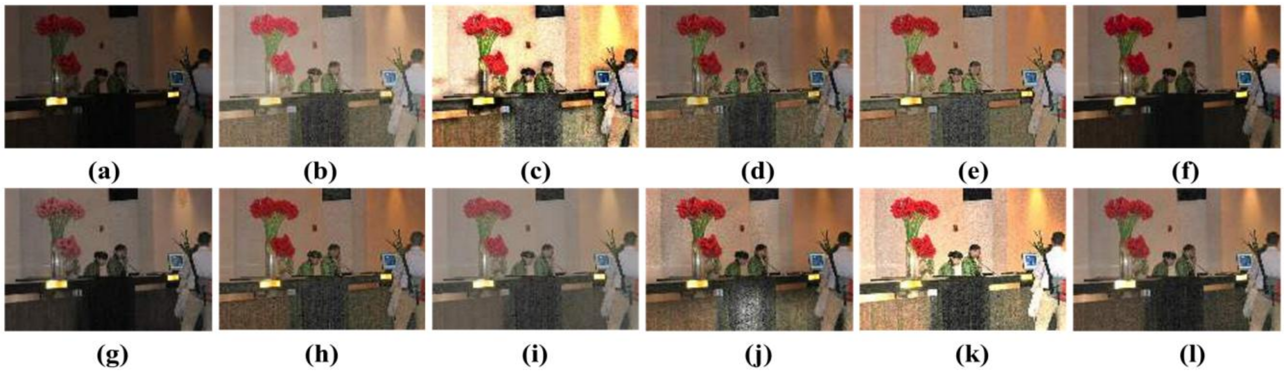

Fig. 14. Comparison outcomes of the ExDark dataset (Batch 5): (a) Original degraded image, (b) ACGC, (c) PLM, (d) FE, (e) AIE, (f) UIE, (g) TS, (h) FBPBF, (i) NCC_PLM, (j) LightenNet, (k) LIME, (l) the proposed RISSR algorithm.

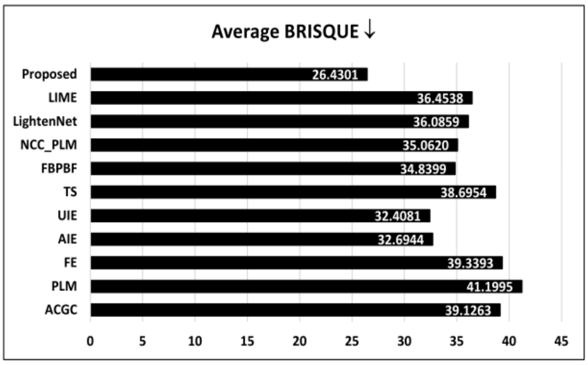

Fig. 15. The average scores of BRISQUE for comparison 1.

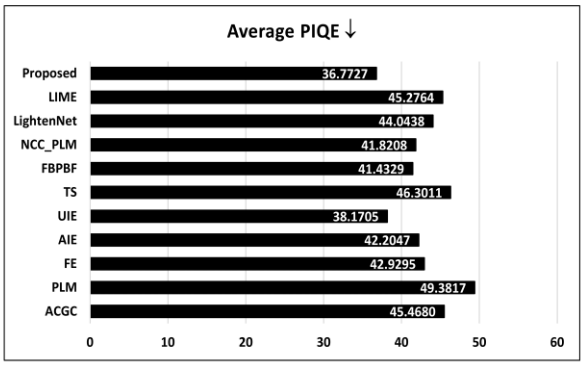

Fig. 16. The average scores of PIQE for comparison 1.

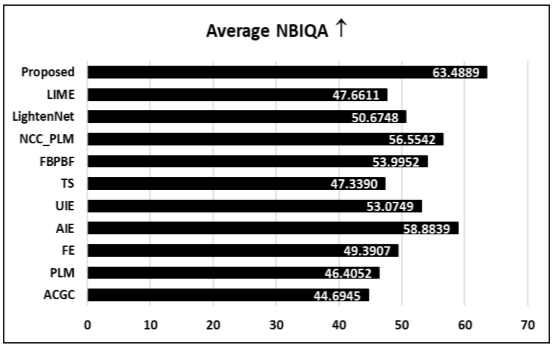

Fig. 17. The average scores of NBIQA for comparison 1.

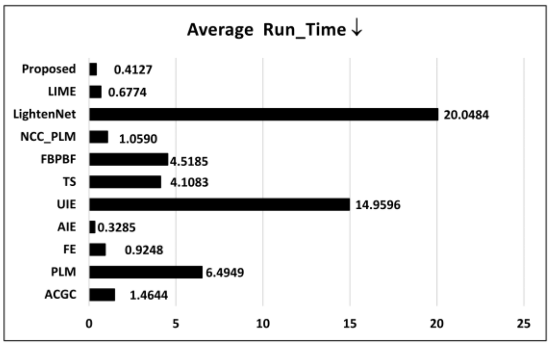

Fig. 18. The average processing-times for comparison 1.

TABLE I. THE RECORDED BRISQUE ↓ SCORES FOR COMPARISON 1

No.	Methods	Fig. 10	Fig. 11	Fig. 12	Fig. 13	Fig. 14	Average
1	ACGC	31.7662	33.5983	47.4637	44.4625	38.3409	39.1263
2	PLM	28.2427	38.8248	45.9800	50.9853	41.9645	41.1995
3	FE	22.9857	31.0562	51.4367	51.8047	39.4133	39.3393
4	AIE	27.0175	23.6121	45.5707	36.3073	30.9645	32.6944
5	UIE	19.8801	20.6607	45.2718	42.4000	33.8280	32.4081
6	TS	24.7864	25.7753	53.0054	45.4816	44.4281	38.6954
7	FBPBF	23.6964	25.2407	45.6192	44.2230	35.4202	34.8399
8	NCC_PLM	23.4013	26.6103	45.4617	42.1370	37.6998	35.0620
9	LightenNet	25.1468	36.9802	43.4554	38.8051	36.0420	36.0859
10	LIME	26.6707	22.4536	43.4876	48.9719	40.6851	36.4538
11	Proposed algorithm	8.7051	10.6863	43.4582	36.6231	32.6776	26.4301

TABLE II. THE RECORDED PIQE ↓ SCORES FOR COMPARISON 1

No.	Methods	Fig. 10	Fig. 11	Fig. 12	Fig. 13	Fig. 14	Average
1	ACGC	18.5803	40.4914	55.4331	57.0898	55.7456	45.4680
2	PLM	32.1249	49.4891	57.1098	49.0630	59.1219	49.3817
3	FE	18.3913	46.7538	53.2126	46.0676	50.2224	42.9295
4	AIE	24.5808	38.7367	49.1316	47.4916	51.0826	42.2047
5	UIE	21.9157	40.1661	34.2808	52.5441	41.9460	38.1705
6	TS	23.4136	44.2777	49.4020	52.6512	61.7611	46.3011
7	FBPBF	19.2576	39.2550	51.6568	46.0305	50.9647	41.4329
8	NCC_PLM	21.4041	37.4885	51.8883	50.0692	48.2540	41.8208
9	LightenNet	26.8532	44.7105	47.6530	51.0883	49.9141	44.0438
10	LIME	29.4294	41.8549	53.3052	48.9006	52.8921	45.2764
11	Proposed algorithm	17.9880	36.8306	34.1680	47.5289	47.3482	36.7727

TABLE III. THE RECORDED NBIQA ↑ SCORES FOR COMPARISON 1

No.	Methods	Fig. 10	Fig. 11	Fig. 12	Fig. 13	Fig. 14	Average
1	ACGC	60.3614	54.6864	37.7801	33.1379	37.5068	44.6945
2	PLM	68.7601	61.8891	40.2411	31.0936	30.0421	46.4052
3	FE	73.8860	62.9991	44.6626	33.3320	32.0740	49.3907
4	AIE	77.5780	60.2944	54.3071	50.2238	52.0161	58.8839
5	UIE	76.9740	57.0947	39.0517	44.2381	48.0161	53.0749
6	TS	74.8152	56.9063	36.4322	32.5678	35.9733	47.3390
7	FBPBF	76.4361	66.0676	42.7549	47.6309	37.0863	53.9952
8	NCC_PLM	77.0546	70.0441	44.2255	43.0595	48.3874	56.5542
9	LightenNet	64.7598	52.9063	48.1769	44.2411	43.2897	50.6748
10	LIME	50.7626	49.5476	51.7924	41.6626	44.5401	47.6611
11	Proposed algorithm	79.6566	70.5420	55.1273	53.3370	58.7818	63.4889

TABLE IV. THE RECORDED PROCESSING-TIME ↓ (IN SECOND)

No.	Methods	Fig.10	Fig. 11	Fig. 12	Fig. 13	Fig. 14	Average
1	ACGC	4.5502	1.6582	0.4199	0.346872	0.346571	1.4644
2	PLM	25.5934	4.9154	0.7019	0.671133	0.592439	6.4949
3	FE	2.3160	0.9211	0.3632	0.726971	0.296574	0.9248
4	AIE	0.9937	0.3906	0.0911	0.093853	0.073423	0.3285
5	UIE	62.2751	10.6217	0.7308	0.608731	0.561872	14.9596
6	TS	12.7585	2.3815	0.1943	2.297865	2.90953	4.1083
7	FBPBF	11.2867	5.7523	3.2433	1.031229	1.278956	4.5185
8	NCC_PLM	3.2490	1.2484	0.2668	0.260707	0.270393	1.0590
9	LightenNet	86.36812	4.5352	3.860591	3.144312	2.333859	20.0484
10	LIME	2.01907	0.679915	0.23884	0.188691	0.260539	0.6774
11	Proposed algorithm	1.0749	0.3563	0.1089	0.05708	0.4663	0.4127

TABLE V. THE AVERAGE SCORES FOR 300 IMAGES IN COMPARISON 1

Metrics	ACGC	PLM	FE	AIE	UIE	TS	FBPBF	NCC_PLM	LightenNet	LIME	Proposed
BRISQUE	44.112	46.185	45.909	36.893	36.394	42.652	37.826	39.047	41.072	42.439	29.416
PIQE	50.455	54.032	47.929	47.855	42.820	50.951	46.083	47.320	48.694	50.163	38.799
NBIQA	45.734	48.374	55.359	64.852	59.043	51.307	61.963	62.523	58.643	52.629	69.857

B. Comparison 2

The second comparison was made on 100 low-light color images from the LOL-v1 dataset, evaluated using two full-reference metrics, PSNR and SSIM. Figs. 19–22 shows the results of visual comparison on the LOL-v1 dataset. Tables VI and VII present the recorded metric scores and Figs. 23 and 24 represent the results as averages in the form of graphs. Table VIII represents the results of 100 images as averages for all algorithms. The ACGC algorithm enhances the illumination of the low-light images in a way that results in washed-out colors and the occurrence of a lot of noise in some images. This justifies it received below high PSNR and a moderate SSIM. While the PLM algorithm produces images with unrealistic colors and halo artifacts. Therefore, it received below moderate in both PSNR and SSIM. As for the FE algorithm, it received the second best in both metrics because the resultant images have good illumination with little noise. The AIE algorithm produced images with appropriate lighting, but it caused a loss of some edge information. It received high scores in PSNR and SSIM. The UIE algorithm failed to light most of the images, which led to invisible image details. This is why it received the worst in PSNR and SSIM. As for the TS algorithm, it received poor in metrics because it shows a dark appearance in the resultant images with unnatural color transitions. The FBPBF algorithm doesn't provide enough lightning, which affects the clarity of details. Therefore, it received a very low PSNR and a low SSIM. The NCC_PLM algorithm results in images with pallid colors. It received above moderate in both metrics. The images produced by the LightenNet algorithm don't have noise, but the images' illumination is still dim. It received low and very low in PSNR and SSIM respectively. The LIME algorithm produced bright artifacts, which led to an unusual appearance. It received a moderate PSNR and a value below high in SSIM. The proposed RISSR algorithm offers satisfactory improvement and appropriate illumination. It provides a more natural appearance and maintains image details without any artifacts or halos appearing. This justifies why it received the best in both metrics.

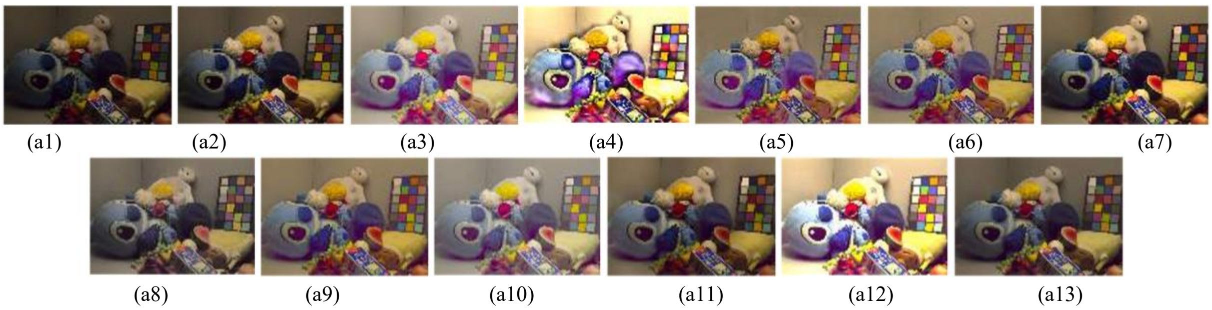

Fig. 19. Comparison outcomes of the LOL-v1 dataset (Batch 1): (a1) Original degraded image, (a2) Ground truth, (a3) ACGC, (a4) PLM, (a5) FE, (a6) AIE, (a7) UIE, (a8) TS, (a9) FBPBF, (a10) NCC_PLM, (a11) LightenNet, (a12) LIME, (a13) the proposed RISSR algorithm.

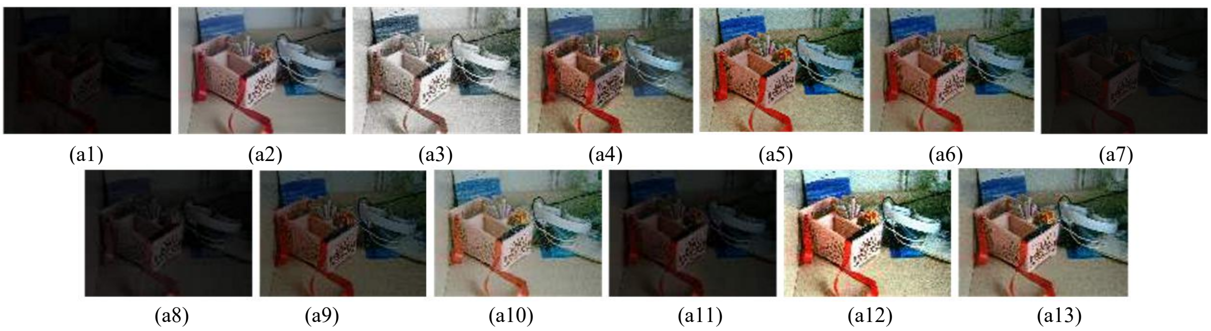

Fig. 20. Comparison outcomes of the LOL-v1 dataset (Batch 2): (a1) Original degraded image, (a2) Ground truth, (a3) ACGC, (a4) PLM, (a5) FE, (a6) AIE, (a7) UIE, (a8) TS, (a9) FBPBF, (a10) NCC_PLM, (a11) LightenNet, (a12) LIME, (a13) the proposed RISSR algorithm.

(a8) (a9) (a10) (a11) (a12) (a13)

Fig. 21. Comparison outcomes of the LOL-v1 dataset (Batch 3): (a1) Original degraded image, (a2) Ground truth, (a3) ACGC, (a4) PLM, (a5) FE, (a6) AIE, (a7) UIE, (a8) TS, (a9) FBPBF, (a10) NCC_PLM, (a11) LightenNet, (a12) LIME, (a13) the proposed RISSR algorithm.

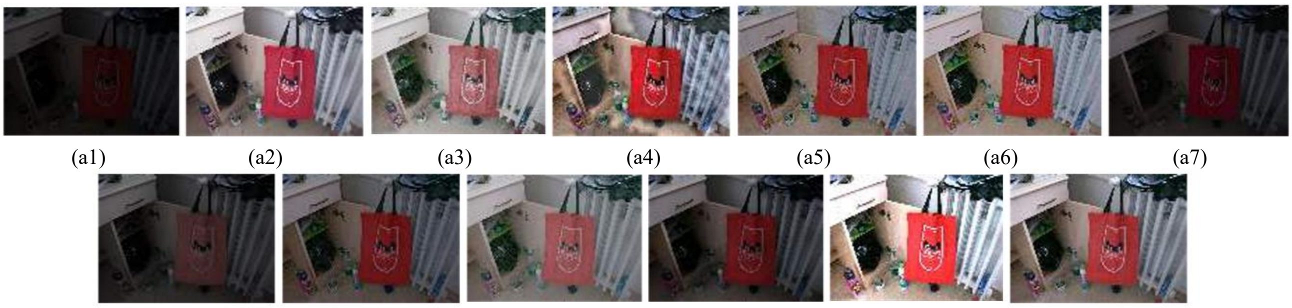

(a1) (a2) (a3) (a4) (a5) (a6) (a7)

(a8) (a9) (a10) (a11) (a12) (a13)

Fig. 22. Comparison outcomes of the LOL-v1 dataset (Batch 4): (a1) Original degraded image, (a2) Ground truth, (a3) ACGC, (a4) PLM, (a5) FE, (a6) AIE, (a7) UIE, (a8) TS, (a9) FBPBF, (a10) NCC_PLM, (a11) LightenNet, (a12) LIME, (a13) the proposed RISSR algorithm.

TABLE VI. THE RECORDED PSNR ↑ SCORES FOR COMPARISON 2

No.	Methods	Fig. 20	Fig. 21	Fig. 22	Fig. 23	Average
1	ACGC	16.8071	15.3263	17.1445	15.0268	16.0762
2	PLM	12.8915	14.6834	12.9921	15.0178	13.8962
3	FE	20.8268	15.5401	21.1068	16.4112	18.4712
4	AIE	19.7271	16.0051	17.1394	14.8295	16.9253
5	UIE	7.0273	5.5638	8.0221	7.9663	7.1449
6	TS	8.8275	8.3393	9.2183	10.9504	9.3339
7	FBPBF	10.2511	9.6941	9.7301	12.0283	10.4259
8	NCC_PLM	16.0221	14.6302	16.9815	15.8723	15.8765
9	LightenNet	13.8521	12.4361	9.2173	12.8329	12.0846
10	LIME	13.9971	16.2863	13.3231	15.7726	14.8448
11	Proposed algorithm	22.8268	15.0310	19.0698	18.9371	18.9662

TABLE VII. THE RECORDED SSIM ↑ SCORES FOR COMPARISON 2

No.	Methods	Fig. 20	Fig. 21	Fig. 22	Fig. 23	Average
1	ACGC	0.4713	0.5016	0.4001	0.5049	0.4695
2	PLM	0.4142	0.4633	0.4702	0.5149	0.4657
3	FE	0.7003	0.6643	0.6298	0.6032	0.6494
4	AIE	0.5901	0.6015	0.5390	0.4982	0.5572
5	UIE	0.7031	0.4042	0.3501	0.3114	0.4422
6	TS	0.6344	0.3955	0.4237	0.3616	0.4538
7	FBPBF	0.6002	0.4171	0.4303	0.4004	0.4620
8	NCC_PLM	0.5601	0.5717	0.4731	0.4299	0.5087
9	LightenNet	0.6273	0.4013	0.4112	0.4071	0.4617
10	LIME	0.5116	0.6371	0.5031	0.4772	0.5323
11	Proposed algorithm	0.8244	0.6736	0.7108	0.7621	0.7427

TABLE VIII. THE AVERAGE SCORES FOR (100) IMAGES IN COMPARISON 2

Metrics	ACGC	PLM	FE	AIE	UIE	TS	FBPBF	NCC_PLM	LightenNet	LIME	Proposed
PSNR	17.052	11.921	19.581	19.028	6.169	7.358	7.876	15.896	10.055	15.820	**22.259**
SSIM	0.4175	0.3895	0.5764	0.5200	0.3667	0.3705	0.3797	0.4051	0.3653	0.5449	**0.7015**

C. Failure Cases

Although the proposed RISSR algorithm showed great enhancement for dim-light images, it demonstrates restricted effectiveness in cases when the degradation arises in image caused by compression artifacts or incorrect contrast. As regards images with incorrect contrast, the resultant images from the RISSR algorithm suffer from limited local contrast. Processing images with compression artifacts results in images with visible blocking artifacts. Fig. 25 shows the failure cases.

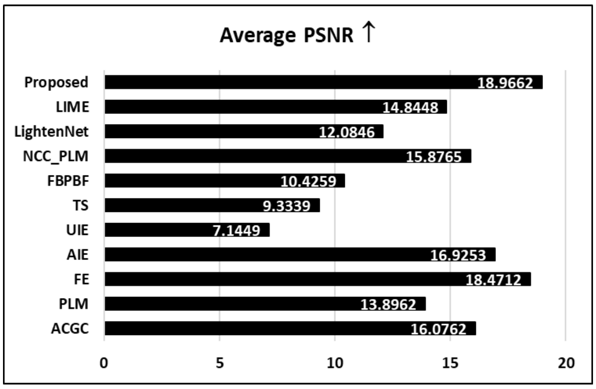

Fig. 23. The average scores of PSNR for comparison 2.

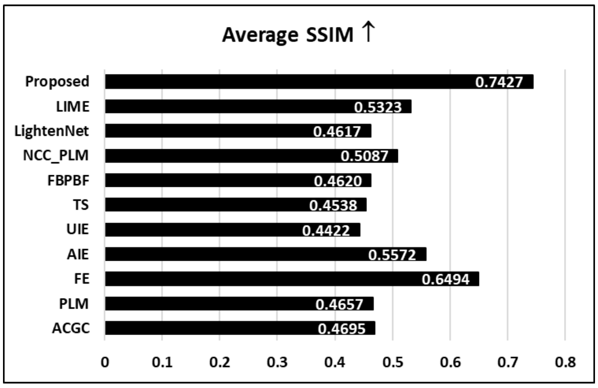

Fig. 24. The average scores of SSIM for comparison 2.

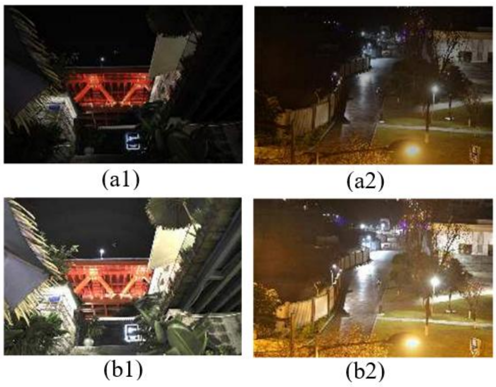

Fig. 25. Failure cases: (a1) compression artifacts, (a2) incorrect contrast, (b1) and (b2) images processed using RISSR.

V. Conclusion

This study presents the proposed RISSR algorithm for improving low-light images. The proposed algorithm is based on Retinex theory and uses the Global Reinhard operator to optimize the image's illumination component, which is used to improve the image's color channels. The level of detail enhancement is adjusted using a gamma correction function followed by a linear scaling function. The performance of the proposed algorithm was tested on a set of actual low-light images, compared with ten other algorithms, and evaluated using five metrics in addition to processing time. The results demonstrated the superiority of the proposed algorithm, its ability to produce images with perceptible quality, good contrast, and adequate brightness without any unwanted artifacts in a better processing time.

Conflict of Interest

The authors declare no conflict of interest.

Author Contributions

Manar A. Al-Abaji has contributed to the study's analysis, research design, data collection, algorithm development and drafting. Mohammed Hazim Alkawaz provided guidance of the used methodology, amendments and data interpretation, algorithm development, analysis of findings; all authors had accepted the final version.

Acknowledgment

The authors are grateful to the College of Education for Pure Science at the University of Mosul in Iraq for their support.

References

[1] K. S. Sundari and B. S. Keerthi, "Enhancing low-light images using Sakaguchi type function and Gegenbauer polynomial," *Sci. Rep.*, vol. 14, no. 1, 29679, 2024. doi: 10.1038/s41598-024-80605-w

[2] M. J. C. S. Reis, "Low-light image enhancement using deep learning: A lightweight network with synthetic and benchmark dataset evaluation," *Appl. Sci.*, vol. 15, no. 11, 6330, 2025. doi: 10.3390/app15116330

[3] A. Patil, T. Chaudhari, K. Deo, K. Sonawane, and R. Bora, "Low light image enhancement for dark images," *Int. J. Data Sci. Anal.*, vol. 6, no. 4, 99, 2020. doi: 10.11648/j.ijdsa.20200604.11

[4] J. Guo, J. Ma, Á. F. García-Fernández, Y. Zhang, and H. Liang, "A survey on image enhancement for low-light images," *Heliyon*, vol. 9, no. 4, e14558, 2023. doi: 10.1016/j.heliyon.2023.e14558

[5] Z. Al-Ameen, "Nighttime image enhancement using a new illumination boost algorithm," *IET Image Process.*, vol. 13, no. 8, pp. 1314–1320, 2019. doi: 10.1049/iet-ipr.2018.6585

[6] G. A. Alhamzawi, A. S. Alfoudi, and A. H. Alsaeedi, "A review of modern low light image enhancement techniques," *Muthanna J. Pure Sci.*, vol. 12, no. 1, pp. 30–48, 2025. doi: 10.52113/2/12.01.2025/30-48

[7] X. Fu, D. Zeng, Y. Huang, Y. Liao, X. Ding, and J. Paisley, "A fusion-based enhancing method for weakly illuminated images," *Signal Processing*, vol. 129, pp. 82–96, 2016. doi: 10.1016/j.sigpro.2016.05.031

[8] S. Yu and H. Zhu, "Low-illumination image enhancement algorithm based on a physical lighting model," *IEEE Trans. Circuits Syst. Video Technol.*, vol. 29, no. 1, pp. 28–37, 2019. doi: 10.1109/TCSVT.2017.2763180

[9] S. Ghosh and K. N. Chaudhury, "Fast bright-pass bilateral filtering for low-light enhancement," in *Proc. 2019 IEEE International Conference on Image Processing (ICIP)*, 2019, pp. 205–209. doi: 10.1109/ICIP.2019.8802986

[10] W. Wang, Z. Chen, X. Yuan, and X. Wu, "Adaptive image enhancement method for correcting low-illumination images," *Inf. Sci. (Ny).*, vol. 496, pp. 25–41, 2019. doi: 10.1016/j.ins.2019.05.015

[11] S. Hao, X. Han, Y. Guo, X. Xu, and M. Wang, "Low-light image enhancement with semi-decoupled decomposition," *IEEE Trans. Multimed.*, vol. 22, no. 12, pp. 3025–3038, 2020. doi: 10.1109/TMM.2020.2969790

[12] M. F. Hassan, "A uniform illumination image enhancement via linear transformation in CIELAB color space," *Multimed. Tools Appl.*, vol. 81, no. 18, pp. 26331–26343, 2022. doi: 10.1007/s11042-022-12429-7

[13] M. F. Hassan, T. Adam, H. Rajagopal, and R. Paramesran, "A hue preserving uniform illumination image enhancement via triangle similarity criterion in HSI color space," *Vis. Comput.*, vol. 39, no. 12, pp. 6755–6766, 2023. doi: 10.1007/s00371-022-02761-2

[14] Y. Demir and N. H. Kaplan, "Low-light image enhancement based on sharpening-smoothing image filter," *Digit. Signal Process.*, vol. 138, 104054, 2023. doi: 10.1016/j.dsp.2023.104054
[15] M. Wang, J. Li, and C. Zhang, "Low-light image enhancement by deep learning network for improved illumination map," *Comput. Vis. Image Underst.*, vol. 232, 103681, 2023. doi: 10.1016/j.cviu.2023.103681
[16] W. Wang, B. Yin, L. Li, L. Li, and H. Liu, "A low light image enhancement method based on dehazing physical model," *Comput. Model. Eng. Sci*., vol. 143, no. 2, pp. 1595–1616, 2025. doi: 10.32604/cmes.2025.063595
[17] N. Severoglu, Y. Demir, N. H. Kaplan, and S. Kucuk, "ACGC: Adaptive chrominance gamma correction for low-light image enhancement," *J. Vis. Commun. Image Represent*., vol. 107, 104402, 2025. doi: 10.1016/j.jvcir.2025.104402
[18] S. Kucuk, N. Severoglu, Y. Demir, and N. H. Kaplan, "New color channel driven physical lighting model for low-light image enhancement," *Digit. Signal Process*., vol. 156, 104757, 2025. doi: 10.1016/j.dsp.2024.104757
[19] E. Reinhard, M. Stark, P. Shirley, and J. Ferwerda, "Photographic tone reproduction for digital images," *ACM Trans. Graph*., vol. 21, no. 3, pp. 267–276, 2002. doi: 10.1145/566654.566575
[20] P. Shirley, A. Robison, and R. K. Morley, "A simple algorithm for managing color in global tone reproduction," *J. Graph. GPU, Game Tools*, vol. 15, no. 3, pp. 199–205, 2011. doi: 10.1080/2151237X.2011.610677
[21] F. Banterle, P. Ledda, K. Debattista, and A. Chalmers, "Inverse tone mapping," in *Proc. the 4th International Conference on Computer Graphics and Interactive Techniques in Australasia and Southeast Asia*, 2006, pp. 349–356. doi: 10.1145/1174429.1174489
[22] D. J. Jobson, Z. Rahman, and G. A. Woodell, "Properties and performance of a center/surround retinex," *IEEE Trans. Image Process.*, vol. 6, no. 3, pp. 451–462, 1997. doi: 10.1109/83.557356
[23] M. A. Al-Hashim and Z. Al-Ameen, "Retinex-based multiphase algorithm for low-light image enhancement," *Trait. du Signal*, vol. 37, no. 5, pp. 733–743, 2020. doi: 10.18280/ts.370505
[24] O. Basheer and Z. Al-Ameen, "Illumination enhancement of nighttime images using a regulated single scale Retinex algorithm," *Jordanian J. Comput. Inf. Technol.*, vol. 10, no. 2, 2024. doi: 10.5455/jjcit.71-1705156218
[25] Q. Xu, S. Jiang, W. Huang, F. Ye, and S. Xu, "Feature fusion based image retrieval using deep learning," *J. Inf. & Computational Sci*., vol. 12, no. 6, pp. 2361–2373, 2015.
[26] M. Iuliani, M. Fontani, and A. Piva, "A leak in PRNU based source identification—questioning fingerprint uniqueness," *IEEE Access*, vol. 9, pp. 52455–52463, 2021. doi: 10.1109/ACCESS.2021.3070478
[27] C. Lee, C. Lee, and C. S. Kim, "Contrast enhancement based on layered difference representation," in *Proc. 2012 19th IEEE International Conference on Image Processing*, 2012, pp. 965–968. doi: 10.1109/ICIP.2012.6467022
[28] K. Ma, K. Zeng, and Z. Wang, "Perceptual quality assessment for multi-exposure image fusion," *IEEE Trans. Image Process*, vol. 24 no. 11, pp. 3345–3356, 2015. doi:10.1109/TIP.2015.2442920
[29] Y. P. Loh and C. S. Chan, "Getting to know low-light images with the exclusively dark dataset," *Computer Vision and Image Understanding*, vol. 178, pp. 30–42, 2019.
[30] C. Wei, W. Wang, W. Yang, and J. Liu, "Deep retinex decomposition for low-light enhancement," arXiv Preprint, arXiv:1808.04560, 2018.
[31] C. Li, J. Guo, F. Porikli, and Y. Pang, "LightenNet: A convolutional neural network for weakly illuminated image enhancement," *Pattern Recognition Letters*, vol. 104, pp. 15–22, 2018. doi: 10.1016/j.patrec.2018.01.010
[32] X. Guo, Y. Li, and H. Ling, "LIME: Low-light image enhancement via illumination map estimation," *IEEE Transactions on Image Processing*, vol. 26, no. 2, pp. 982–993, 2016.
[33] T. Sun, X. Zhu, J. S. Pan, J. Wen, and F. Meng, "No-reference image quality assessment in spatial domain," *Advances in Intelligent Systems and Computing*, vol. 329, pp. 381–388, 2015. doi: 10.1007/978-3-319-12286-1_39
[34] N. Venkatanath, D. Praneeth, S. C. Sumohana, and S. M. Swarup, "Blind image quality evaluation using perception based features," in *Proc. 2015 Twenty First National Conference on Communications (NCC)*, 2015, pp. 1–6. doi: 10.1109/NCC.2015.7084843
[35] F. Z. Ou, Y. G. Wang, and G. Zhu, "A novel blind image quality assessment method based on refined natural scene statistics," in *Proc. 2019 IEEE International Conference on Image Processing (ICIP)*, 2019, pp. 1004–1008. doi: 10.1109/ICIP.2019.8803047
[36] Z. Wang, A. C. Bovik, H. R. Sheikh, and E. P. Simoncelli, "Image quality assessment: From error visibility to structural similarity," *IEEE Trans. IMAGE Process*., vol. 13, no. 4, pp. 600–612, 2004. doi: 10.1109/TIP.2003.819861